Helical Structures Hot Paper

How to cite:
International Edition: doi.org/10.1002/anie.202217325
German Edition: doi.org/10.1002/ange.202217325

Homochiral versus Heterochiral Dimeric Helical Foldamer Bundles: Chlorinated-Solvent-Dependent Self-Sorting

*Friedericke S. Menke, Barbara Wicher, Victor Maurizot, and Ivan Huc**

Abstract: Aromatic oligoamide sequences programmed to fold into stable helical conformations were designed to display a linear array of hydrogen-bond donors and acceptors at their surface. Sequences were prepared by solid-phase synthesis. Solution ^{1}H NMR spectroscopic studies and solid-state crystallographic structures demonstrated the formation of stable hydrogen-bond-mediated dimeric helix bundles that could be either heterochiral (with a *P* and an *M* helix) or homochiral (with two *P* or two *M* helices). Formation of the hetero- or homochiral dimers could be driven quantitatively using different chlorinated solvents—exemplifying a remarkable case of either social or narcissistic chiral self-sorting or upon imposing absolute handedness to the helices to forbid *PM* species.

The bundling of α-helices mediated by hydrophobic residues, charge-reinforced hydrogen bonds, or metal ion coordination in water is the best understood assembly mode of protein secondary structural motifs. It is amenable to design and has found applications in multiple contexts.[1] It has, for example, been extended to α-peptide 3_{10} helices,[2] α/β-peptides,[3] β-peptides[4] and oligourea foldamers.[5] A general feature of peptide helix bundling is the homochiral nature of the helices, which eventually gives rise to coil-coiling, that is, the winding of helices around one another. Certain amino acid patterns have also been found to allow for bundling between L- and D-peptide helices.[6] The opposite handedness of the helices then leads to strictly parallel[7] arrangements, namely without coiling of the coils.

In the context of a program aiming at producing abiotic protein-like tertiary structures, we have explored the extension of helix bundling to organic solvents using aromatic foldamer helices. Starting from the structurally well-defined 2.5 helices formed by oligoamides of δ-amino acids Q and P (Figure 1a),[8] we have introduced analogous hydroxy-functionalized X and Y monomers to create arrays of helix-to-helix hydrogen bonds between hydroxy donors and amide carbonyl acceptors. For example, when connected by a rigid linker at their C-terminus, sequences **1** and **2** form homochiral head-to-head helix-turn-helix structures stabilized by X···X and Y···Y hydrogen bonding (Figure 1c).[9] Using an N-to-C helix connection with another linker, a similar, albeit heterochiral and head-to-tail, helix-turn-helix structure was generated.[9c] However, in the absence of a linker, helices of **1** and **2** assemble into several types of aggregates, including tilted dimers in which helix axes form an angle of ≈60°, as well as trimers with all helices parallel[7] with a head-to-head arrangement of the oligomers (Figure S1).[9a] In most cases, different aggregates were found to coexist in solution. In search for better-behaved helix bundling by self-assembly, i.e. not guided by a rigid linker, we have now explored and report on the aggregation behavior of sequences **3**–**7**, where Y units have been replaced by P. These helices thus only contain X hydrogen-bond donors located every five units, that is, every other helix turn, so as to form a linear array (Figure 1d). This design was motivated by the key role played by Y units in the above-mentioned aggregates (Figure S1): it was expected that removing them would change the aggregation behavior and also that long helices would favor parallel,[7] as opposed to tilted, arrangements of helix axes. Besides, helix-turn-helix folding has been shown to occur without any Y units.[10]

Here, we report that the new sequences may form homo- or heterochiral helix dimers mediated by a new array of hydrogen bonds. Furthermore, we found that dimer formation strongly depends on the chlorinated solvent used, namely chloroform [$CDCl_3$], tetrachloroethane [$(CDCl_2)_2$], dichloromethane [CD_2Cl_2], and dichloroethane [$(CD_2Cl)_2$]. Thus, hetero- vs. homochiral helix association can be quantitatively reverted by changes in the solvent nature as small as going from $CDCl_3$ to CD_2Cl_2. Our results thus not only delivered new robust aggregation modes that can serve for future abiotic tertiary and quaternary structure design, but also the possibility to switch them. They also highlight large amplitude chlorinated solvent effects that raise questions about their generality.

[*] F. S. Menke, Prof. I. Huc
Department of Pharmacy, Ludwig-Maximilians-University of Munich
Butenandtstr. 5–13, 81377 München (Germany)
E-mail: ivan.huc@cup.lmu.de

Dr. B. Wicher
Department of Chemical Technology of Drugs, Poznan University of Medical Sciences
6 Grunwaldzka St., 60-780 Poznan (Poland)

Dr. V. Maurizot
CBMN (UMR 5248), Univ. Bordeaux, CNRS, Bordeaux INP
2, Rue Robert Escarpit, 33600 Pessac (France)

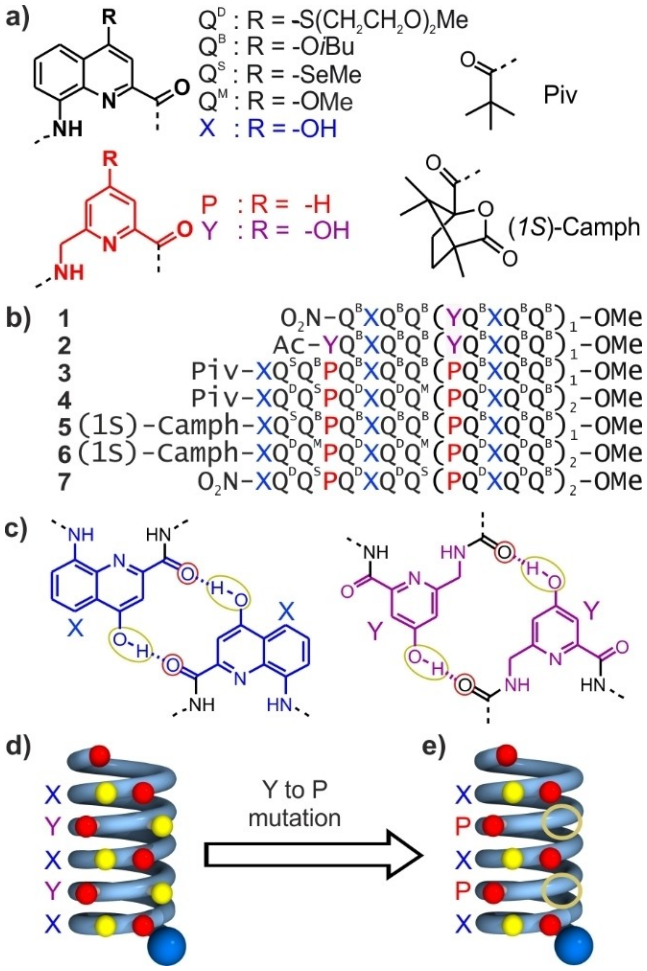

Figure 1. a) Structures of units Q, X, P and Y, amino acid monomers as well as N-terminal piv and (1*S*)-camph groups. Q^D and Q^B carry organic solubilizing side chains. Q^S was introduced in some sequences to assist crystallographic structure elucidation through the anomalous scattering of Se, although it turned out to be unneeded. Q^M is isosteric to Q^S. b) Oligoamide foldamer sequences. In sequences ending with an 8-nitro group, this group replaces the terminal amine. c) Hydrogen-bonding patterns involving X and Y units as observed in tertiary structures in which sequences **1** or **2** are connected by a linker at their C-terminus.[9a,c] d,e) Schematic representation of the positioning of hydrogen-bond donors (yellow balls) and acceptors (red balls) at the surface of a helix containing X and Y (d) or X and P (e). The N-terminus is marked with a blue ball.

Sequence **3** and its extended version **4** were synthesized (see Supporting Information for details). Their ^{1}H NMR spectra in $CDCl_3$ show a single set of sharp resonances (Figure 2a). The signals of OH protons could be identified as being exchangeable with deuterium and not correlated to nitrogen in $^1H^{15}N$-HSQC spectra (Figures S2, S3). The chemical shift values >9 ppm of the OH protons indicated their involvement in hydrogen bonding, i.e. the formation of aggregates. The multiplicity of NMR signals showed that all the helices within the aggregate are in an identical environment, implying that the aggregate must be symmetrical. A solid-state structure of **3** was then obtained[11] that revealed a new head-to-tail dimeric arrangement held together by six very similar intermolecular hydrogen bonds arranged in a linear array (Figure S4). Attempts to crystallize **4** were unsuccessful, but its nitro-terminated analogue **7** crystallized, and its solid-state structure revealed the very same pattern as **3** extended to eight intermolecular hydrogen bonds (Figure 3a, b).[11] The conservation of the pattern for different helix lengths indicates it is robust. In both cases, the helix axes are parallel,[7] and the dimer is heterochiral (*meso*)—it involves a *P* helix and an *M* helix—and is nearly (not crystallographically) centrosymmetric and thus, in those cases, achiral. Hydrogen bonds occur between hydroxy groups of X units of one helix and amide carbonyl groups preceding P units of the other helix or the ester carbonyl at the C-terminus (Figure 3c). This contrasts with earlier parallel aggregates involving X···X and Y···Y hydrogen bonding (Figure 1c). Because the helices are now shifted (or out of register) by one helix turn with respect to earlier parallel aggregates, and the X-units no longer face each other, we called these new aggregates *PM* (or heterochiral) *shifted* dimers. Using molecular models, we could build alternate plausible hydrogen-bond arrays between *P* and *M* helices, including one non-shifted dimer involving X···X hydrogen bonding, but these must be less stable (Figure S5, see Supporting Information for details). Dilution studies (down to 0.15 mM) led to no visible change in the ^{1}H NMR spectra of **3** and **4** suggesting a tight association in $CDCl_3$. However, *PM* shifted dimers can be dissociated upon adding DMSO-d_6 (Figures S6, S7). Slow exchange on the NMR time scale between monomer and dimer is then observed. A dilution study in 9:1 $CDCl_3$/DMSO-d_6 gave a K_d of 62 μM at 25 °C in this solvent. *PM* shifted dimers thus represent a novel and robust form of heterochiral social self-sorting.[12]

The *PM* shifted dimers were replaced by another species in slow exchange on the NMR timescale upon adding CD_2Cl_2 (Figure 2b, S8, S9). In pure CD_2Cl_2, the replacement is quantitative for **4**. The replacement by the same species was quantitative for both **3** and **4** in $(CD_2Cl)_2$ or toluene-d_8 (Figures S10–S12). In $(CDCl_2)_2$, both species coexisted for **3** (Figure S13). Upon changing the solvent, equilibration sometimes took multiple days and care was taken to ascertain that samples had reached thermodynamic equilibrium (Figures S14, S15, see Supporting Information for details). The proportions between the two species in solvent where they coexist did not depend on concentration, suggesting that both are dimers (from 2.4 to 0.1 mM, Figure S16). They did not change upon heating up to 110 °C either (Figure S17). Consistently, a DOSY spectrum of **3** in CD_2Cl_2 showed that the new aggregate has the same hydrodynamic radius as the *PM* shifted dimers (Figure S18). Signal multiplicity again indicated that the new dimer must have some sort of symmetry and $^1H^{15}N$-HSQC spectra in several solvents confirmed that, in all cases, hydroxy protons resonances were downfield-shifted, indicating their involvement in hydrogen bonds (Figures S19–21). We also noted that the chemical shift values of OH protons had similar patterns in the two dimers, with one signal at a slightly higher field (near 9.2 ppm in $CDCl_3$ and 8.9 ppm in CD_2Cl_2, see below for a tentative assignment) and other signals clustered above 9.5 ppm, hinting at some structural similar-

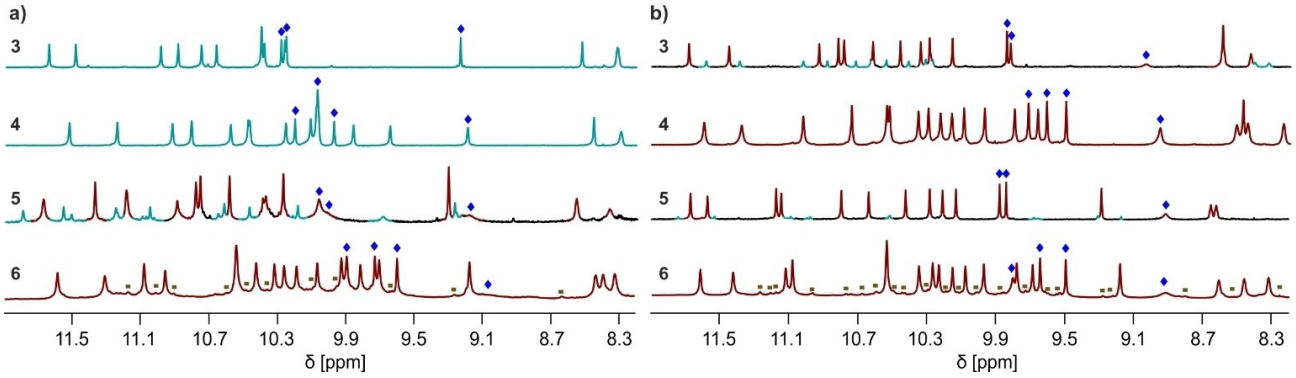

Figure 2. Extracts of the 500 MHz ^{1}H NMR spectra of **3–6** at 2.4 mM in $CDCl_3$ (a) and CD_2Cl_2 (b) at 25 °C showing the amide and hydrogen-bonded OH proton resonances. Signals assigned to OH protons are marked with a blue diamond. Signals assigned to the *PM* shifted dimer and to the chiral shifted dimer are shown in turquoise and in brown, respectively. Impurities in the spectra of **6** are marked with brown squares.

ity. Dilution studies (down to 0.1 mM) showed no sign of dissociation of the new dimer. Measuring an association constant in CD_2Cl_2/DMSO-d_6 mixtures was hampered by the fact that DMSO-d_6 also promoted the formation of the *PM* shifted dimer.

Attempts to crystallize the new dimers of **3** and **4** were unsuccessful, but their nature could be unraveled by studying **5** and **6**, the analogues of **3** and **4** bearing a (1*S*)-camphanyl group at their N-terminus. This modification has been shown to quantitatively (as far as an NMR can detect) bias the handedness of Q_n helices to right-handed (*P*).[13] Sequences **5** and **6** were thus expected to be unable to form *PM* shifted dimers. Indeed, a solid-state structure of **5** was elucidated from a single crystal grown from CH_2Cl_2,[11] showing a nearly C_2-symmetrical parallel[7] head-to-tail homochiral (*PP*) dimer (Figure 3d–f). As in the *PM* shifted dimer, a linear and regular array of six hydrogen bonds is formed between hydroxy protons on one helix and the carbonyl preceding a P unit on the other helix. By analogy, we called this type of dimer a *PP* (or *MM*, homochiral) shifted dimer. Again, we could build energy-minimized models of plausible alternate hydrogen-bond-mediated homochiral helix bundles, but these must be less stable (Figure S22). Differences between the *PM* and *PP*/*MM* shifted dimers are highlighted in Figures 3a–3h, S23 and in Tables S1–S4. The main differences concern symmetry and the orientation of the hydrogen bonds, but the two types of dimers are overall similar. Compounds **3** and **4** exist as racemic mixtures of *P*- and *M*-helical conformers, and thus may also form *PP*/*MM* shifted dimers. Their social self-sorting behavior in $CDCl_3$ is all the more remarkable.

The ^{1}H NMR spectra of **5** and **6** in CD_2Cl_2 are quite similar to those of **3** and **4** (Figures 2b, S24, and S25). In the case of **5**, a second species is present in small amounts similar to the *PM* shifted dimer found in the spectrum of **3**. The proportion of this minor species increases in $CDCl_3$ (Figures 2a, 2b, S26) and the species is absent in $(CD_2Cl)_2$ and toluene-d_8 (Figures S27–S29). In contrast, the spectra of **6** in CD_2Cl_2 shows one species only, which we presume to be a *PP* shifted dimer, and the same species is present in $CDCl_3$ or any $CDCl_3$/CD_2Cl_2 mixture (Figure S30). The (1*S*)-camphanyl group of **6** thus plays its role and *PM* shifted dimer formation is prevented in the absence of *M* helix. We surmised that the second set of signals in the spectra of **5** in $CDCl_3$ and CD_2Cl_2 could be *PM* shifted dimers counteracting the effect of the camphanyl group in a sort of mismatched stereochemical pairing.[14] We then measured the circular dichroism (CD) spectra of **5** in these two solvents and observed a reduced intensity in $CDCl_3$ (Figure S31). The change in intensity matched with the change of proportion measured by NMR. No change in CD intensity was observed with the helical precursor of **5** in which X units are protected as *t*Bu ethers. Furthermore, a second solid-state structure of **5** could be obtained from a single crystal grown from $CHCl_3$. The structure revealed a *PM* shifted dimer extremely similar to that of **3** (Figure S4).[11] This dimer has a *P* and an *M* helix but is not centrosymmetrical: since both helices carry the same (1*S*)-camphanyl group, it is an overall chiral species. In short, the *PM* shifted dimer has such a considerable stability in $CHCl_3$ that, at least in the case of **5**, it partly counteracts the handedness control of the (1*S*)-camphanyl group. Given the behavior of **5** and **6**, we think it reasonable to assign the dimers of **3** and **4** that prevail in CD_2Cl_2, $(CDCl_2)_2$, and toluene-d_8 to *PP*/*MM* shifted dimers, exemplifying strong chiral narcissistic self-sorting in these solvents.[12]

The quantitative reversal of self-sorting of the *P* and *M* helices of **3** and **4** in solution at thermodynamic equilibrium in solvents as similar as $CDCl_3$, which favors social self-sorting, and, for example, $(CD_2Cl)_2$, which favors narcissistic self-sorting is, to the best of our knowledge, unprecedented.[12f,g] We carefully examined the structural parameters of the two types of shifted dimers in the solid-state structures of **3** and **5** (Tables S1–S4) and found no major differences. In both cases, top views of the structure show that helix curvature does not significantly deviate from the preferred 2.5 units per turn (Figure S32). Helix bundling does not generate any apparent strain.[10] In both cases also, a certain degree of steric complementarity is observed like the knobs-into-holes complementarity of peptide helix bundles. Specifically, steric clashes would result from replacing the P units by Q monomers because of the

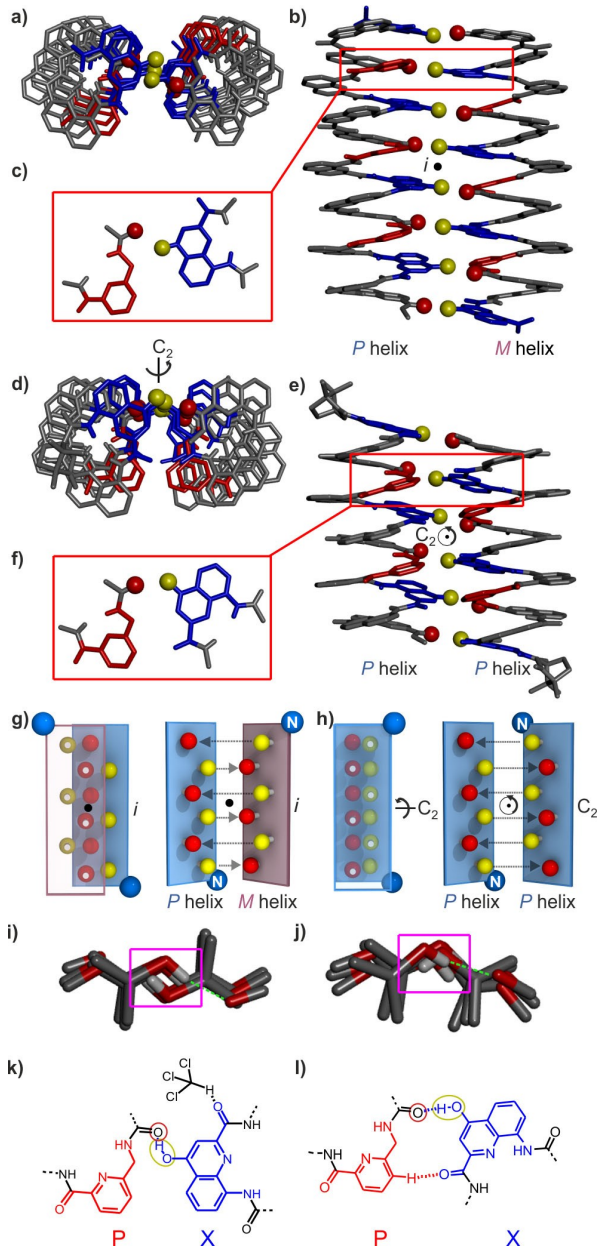

Figure 3. Top view (a), side view (b), and hydrogen-bonding pattern (c) of the crystal structure of the *PM* shifted dimer of **7** that prevails in $CHCl_3$. Top view (d), side view (e) and hydrogen-bonding pattern (f) of the crystal structure of the *PP* shifted dimer of **5** that prevails in CH_2Cl_2. The pseudo-inversion center is indicated by *i*, and the pseudo-twofold axis by C_2. In (a–f) hydroxy and carbonyl oxygen atoms of the hydrogen-bonding arrays are shown as yellow and red balls, respectively. The X and P units are shown in blue and red tubes, respectively. Included solvent molecules, hydrogen atoms and side chains are omitted for clarity. g) Schematic representations of the hydrogen-bonding array of the structure shown in (a–c): overlaid view (left) and open-book view (right; see Figure S23 for details). h) Schematic representations of the hydrogen-bonding array of the structure shown in (d–f): overlaid view (left) and open-book view (right). i) Top view of the hydrogen-bond array of the structure shown in (a). The pink box highlights that local dipoles associated with OH groups are anti-parallel. j) Top view of the hydrogen-bond array of the structure shown in (d). The pink box highlights that local dipoles associated with OH groups are not cancelling each other. k) Typical solvation by $CHCl_3$ molecules of the structure shown in (a–d). l) CH···O=C contact of the structure shown in (d–f) that prevents solvation as in (k).

additional benzenic ring of the latter. In both cases again, the hydrogen bond involving the N-terminal. X unit of one helix and the C-terminal ester carbonyl of the other unit is a little longer than other hydrogen bonds, in agreement with one OH resonance being a little less downfield-shifted than the others (Figure 2). The angles formed by C and O atoms in the COH···O=C hydrogen bonds are not the same in the *PM* and chiral dimers, reflecting a different orientation of OH and carbonyl groups (Figures 3i–3l). In the *PM* dimers, the center of symmetry leads to a better cancellation (anti-parallel arrangement) of local dipoles than in the C_2-symmetrical chiral dimer in which an additive parallel component of the OH dipoles along the C_2 axis can be noted. We thus considered that solvent polarity could influence the relative stability of the two dimers. However, no descriptor of solvent polarity provided a trend that would match with proportions observed experimentally. For example, relative permittivities increase from $CDCl_3$, to $(CDCl_2)_2$, CD_2Cl_2 and $(CD_2Cl)_2$ ($\varepsilon_r = 4.81$, 8.42, 8.93 and 10.36, respectively),[15] which would fit our observations, but toluene-d_8 would then be an outlier ($\varepsilon_r = 2.38$).[16] A possible source of the effect may be solvent acidity, i.e. hydrogen-bonding ability, in particular to the multiple amide carbonyl groups at the surface of helices. Indeed, the solid-state structures of the *PM* shifted dimers of **3**, **5** and **7** contain numerous $CHCl_3$ molecules almost all of which establish Cl_3CH···O=C contacts (Figures 3k, S33). In contrast, the CH_2Cl_2 molecules in the structure of the *PP* dimer of **5** do not play this role (Figure S33). Instead, some amide carbonyl groups are involved in CH···O=C contacts in the chiral dimer structure and are thus unavailable to interact with the solvent (Figure 3d, 3l). This does not occur in the *PM* dimers in which all carbonyl groups, not hydrogen bonded to hydroxy groups are available for interactions with an acidic proton of the solvent. Such different roles of $CHCl_3$ and CH_2Cl_2 in solvation have been documented for when these solvent molecules are included in solid-state structures.[17] However, the effects in solution and their potential amplitude remain unclear. It is also unclear how these effects may vary as a function of helix length. For the shorter helices **3** and **5**, the *PM* shifted dimer shows such stability that it does not completely disappear in CD_2Cl_2 (it does in $(CD_2Cl)_2$), and it partly counteracts the effect of the camphanyl group, whereas the longer helices **4** and **6** are better behaved. Solvent effects as strong as those we report may also influence some of the innumerable hydrogen-bonded assemblies in chlorinated solvents described in the literature. Yet we found no such report.

In conclusion, we have described the formation of stable and well-defined helix bundles of aromatic foldamer helices mediated by new linear arrays of hydrogen bonds, adding to the rich literature on helical molecules and their properties.[18] The spatial organization of the hydrogen-bond donors and acceptors in the helix bundles contrast greatly with tape-like or flat rigid structures presented in other contexts.[19] Helix bundling was shown to undergo a quantitative reversal of self-sorting from social heterochiral (*meso*) to narcissistic homochiral depending on the chlorinated solvent used. The reason why similar solvents may

give rise to such large effects will warrant further investigation. Nevertheless, the new bundles, as well as their amenability to solvent-induced reconstitution, can already serve as building blocks to further elaborate tertiary and quaternary abiotic foldamers. Work along these lines is in progress in our laboratories and will be reported in due course.

Acknowledgements

This work was supported by the DFG (Excellence Cluster 114, CIPSM). M. Palchyk and D. Gill are gratefully acknowledged for contributing synthetic precursors. We also thank D. Gill and D. Bindl for monomer synthesis, L. Allmendinger and C. Glas for assistance with NMR measurements, and B. Kauffmann for crystallographic data collection. This work has benefited from the facilities and expertise of the Biophysical and Structural Chemistry platform (BPCS) at IECB, CNRS UMS3033, Inserm US001, and Bordeaux University. Open Access funding enabled and organized by Projekt DEAL.

Conflict of Interest

The authors declare no conflict of interest.

Data Availability Statement

The data that support the findings of this study are available from the corresponding author upon reasonable request.

Keywords: Chlorinated Solvents · Foldamer · Helix Bundling · Hydrogen Bonding · Self-Sorting

[1] a) C. W. Wood, D. N. Woolfson, *Protein Sci.* **2018**, *27*, 103–111; b) F. Thomas, W. M. Dawson, E. J. M. Lang, A. J. Burton, G. J. Bartlett, G. G. Rhys, A. J. Mulholland, D. N. Woolfson, *ACS Synth. Biol.* **2018**, *7*, 1808–1816; c) G. G. Rhys, J. A. Cross, W. M. Dawson, H. F. Thompson, S. Shanmugaratnam, N. J. Savery, M. P. Dodding, B. Höcker, D. N. Woolfson, *Nat. Chem. Biol.* **2022**, *18*, 999–1004; d) A. J. Scott, A. Niitsu, H. T. Kratochvil, E. J. M. Lang, J. T. Sengel, W. M. Dawson, K. R. Mahendran, M. Mravic, A. R. Thomson, R. L. Brady, L. Liu, A. J. Mulholland, H. Bayley, W. F. Degrado, M. I. Wallace, D. N. Woolfson, *Nat. Chem.* **2021**, *13*, 643–650; e) M. J. Chalkley, S. I. Mann, W. F. Degrado, *Nat. Chem. Rev.* **2022**, *6*, 31–50; f) M. Mravic, J. L. Thomaston, M. Tucker, P. E. S. Lijun Liu, W. F. Degrado, *Science* **2019**, *363*, 1418–1423; g) F. Pirro, N. Schmidt, J. Lincoff, Z. X. Widel, N. F. Polizzi, L. Liu, M. J. Therien, M. Grabe, M. Chino, A. Lombardi, W. F. Degrado, *Proc. Natl. Acad. Sci. USA* **2020**, *117*, 33246–33253; h) T. Lebar, D. Lainšček, E. Merljak, J. Aupič, R. Jerala, *Nat. Chem. Biol.* **2020**, *16*, 513–519; i) F. Lapenta, J. Aupič, M. Vezzoli, Ž. Strmšek, S. Da Vela, D. I. Svergun, J. M. Carazo, R. Melero, R. Jerala, *Nat. Commun.* **2021**, *12*, 939; j) F. Lapenta, J. Aupič, Ž. Strmšek, R. Jerala, *Chem. Soc. Rev.* **2018**, *47*, 3530–3542.

[2] P. Kumar, N. G. Paterson, J. Clayden, D. N. Woolfson, *Nature* **2022**, *607*, 387–392.

[3] W. S. Horne, J. L. Price, J. L. Keck, S. H. Gellman, *J. Am. Chem. Soc.* **2007**, *129*, 4178–4180.

[4] a) E. J. Petersson, C. J. Craig, D. S. Daniels, J. X. Qiu, A. Schepartz, *J. Am. Chem. Soc.* **2007**, *129*, 5344–5345; b) D. S. Daniels, E. J. Petersson, J. X. Qiu, A. Schepartz, *J. Am. Chem. Soc.* **2007**, *129*, 1532–1533.

[5] a) G. W. Collie, K. Pulka-Ziach, C. M. Lombardo, J. Fremaux, F. Rosu, M. Decossas, L. Mauran, O. Lambert, V. Gabelica, C. D. Mackereth, G. Guichard, *Nat. Chem.* **2015**, *7*, 871–878; b) G. W. Collie, R. Bailly, K. Pulka-Ziach, C. M. Lombardo, L. Mauran, N. Taib-Maamar, J. Dessolin, C. D. Mackereth, G. Guichard, *J. Am. Chem. Soc.* **2017**, *139*, 6128–6137.

[6] a) D. E. Mortenson, J. D. Steinkruger, D. F. Kreitler, D. V. Perroni, G. P. Sorenson, L. Huang, R. Mittal, H. G. Yun, B. R. Travis, M. K. Mahanthappa, K. T. Forest, S. H. Gellman, *Proc. Natl. Acad. Sci. USA* **2015**, *112*, 13144–13149; b) D. F. Kreitler, Z. Yao, J. D. Steinkruger, D. E. Mortenson, L. Huang, R. Mittal, B. R. Travis, K. T. Forest, S. H. Gellman, *J. Am. Chem. Soc.* **2019**, *141*, 1583–1592.

[7] Throughout the manuscript, the term "parallel" refers to helical axes having a parallel orientation without prejudice of the head-to-head or head-to-tail realtive arrangement of the oligoamide chains. The term "anti-parallel" is avoided.

[8] a) H. Jiang, J.-M. Léger, I. Huc, *J. Am. Chem. Soc.* **2003**, *125*, 3448–3449; b) D. Sánchez-García, B. Kauffmann, T. Kawanami, H. Ihara, M. Takafuji, M.-H. Delville, I. Huc, *J. Am. Chem. Soc.* **2009**, *131*, 8642–8648; c) T. Qi, V. Maurizot, H. Noguchi, T. Charoenraks, B. Kauffmann, M. Takafuji, H. Ihara, I. Huc, *Chem. Commun.* **2012**, *48*, 6337; d) F. Devaux, X. Li, D. Sluysmans, V. Maurizot, E. Bakalis, F. Zerbetto, I. Huc, A.-S. Duwez, *Chem* **2021**, *7*, 1333–1346.

[9] a) S. De, B. Chi, T. Granier, T. Qi, V. Maurizot, I. Huc, *Nat. Chem.* **2018**, *10*, 51–57; b) D. Mazzier, S. De, B. Wicher, V. Maurizot, I. Huc, *Chem. Sci.* **2019**, *10*, 6984–6991; c) D. Mazzier, S. De, B. Wicher, V. Maurizot, I. Huc, *Angew. Chem. Int. Ed.* **2020**, *59*, 1606–1610; *Angew. Chem.* **2020**, *132*, 1623–1627.

[10] F. S. Menke, D. Mazzier, B. Wicher, L. Allmendinger, B. Kauffmann, V. Maurizot, I. Huc, *Org. Biomol. Chem.* **2023**, https://doi.org/10.1039/D2OB02109A.

[11] Deposition numbers 2209189 (**3**, racemic); 2209187 (**5**, homochiral); 2209188 (**7**, racemic); 2209186 (**5**, pseudo-racemic) contain the supplementary crystallographic data for this paper. These data are provided free of charge by the joint Cambridge Crystallographic Data Centre and Fachinformationszentrum Karlsruhe Access Structures service.

[12] a) Y. Z. C. Li, Y.-Q. Zhao, S. Zhang, *Chem. Lett.* **2020**, *49*, 1356–1366; b) H. Jędrzejewska, A. Szumna, *Chem. Rev.* **2017**, *117*, 4863–4899; c) T. Koga, M. Matsuoka, N. Higashi, *J. Am. Chem. Soc.* **2005**, *127*, 17596–17597; d) A. Wu, L. Isaacs, *J. Am. Chem. Soc.* **2003**, *125*, 4831–4835; *Angew. Chem. Int. Ed.* **2002**, *41*, 4028–4031; *Angew. Chem.* **2002**, *114*, 4200–4203; e) A. Wu, A. Chakraborty, J. C. Fettinger, R. A. Flowers II, L. Isaacs, *Angew. Chem. Int. Ed.* **2002**, *41*, 4028–4031; *Angew. Chem.* **2002**, *114*, 4200–4203; f) D. Beaudoin, F. Rominger, M. Mastalerz, *Angew. Chem. Int. Ed.* **2017**, *56*, 1244–1248; *Angew. Chem.* **2017**, *129*, 1264–1268; g) P. Wagner, F. Rominger, W. S. Zhang, J. H. Gross, S. M. Elbert, R. R. Schröder, M. Mastalerz, *Angew. Chem. Int. Ed.* **2021**, *60*, 8896–8904; *Angew. Chem.* **2021**, *133*, 8978–8986.

[13] A. M. Kendhale, L. Poniman, Z. Dong, K. Laxmi-Reddy, B. Kauffmann, Y. Ferrand, I. Huc, *J. Org. Chem.* **2011**, *76*, 195–200.

[14] a) X. Sun, W. Li, L. Zhou, X. Zhang, *Chem. Eur. J.* **2009**, *15*, 7302–7305; b) H. B. Jang, Y. R. Choi, K.-S. Jeong, *J. Org. Chem.* **2018**, *83*, 5123–5131.
[15] a) I. G. Tironi, W. F. Van Gunsteren, *Mol. Phys.* **1994**, *83*, 381–403; b) C. Wohlfarth in *Static Dielectric Constants of Pure Liquids and Binary Liquid Mixtures*, Supplement to IV/6M (Ed: M. D. Lechner), Springer-Verlag, Berlin, Heidelberg, **2008**; c) J. Nath, S. K. Chaudhary, *J. Chem. Eng. Data* **1992**, *37*, 387–390.
[16] U. V. Mardolcar, C. A. Nieto de Castro, F. J. V. Santos, *Fluid Phase Equilibria; Dielectric constant measurements of toluene and benzene, Vol. 79*, Elsevier, Aubiere, France, **1992**.
[17] F. H. Allen, P. A. Wood, P. T. A. Galek, *Acta Crystallogr. Sect. B* **2013**, *69*, 379–388.
[18] E. Yashima, N. Ousaka, D. Taura, K. Shimomura, T. Ikai, K. Maeda, *Chem. Rev.* **2016**, *116*, 13752–13990.
[19] a) B. Gong, *Acc. Chem. Res.* **2012**, *45*, 2077–2087; b) D. A. Leigh, C. C. Robertson, A. M. Z. Slawin, P. I. T. Thomson, *J. Am. Chem. Soc.* **2013**, *135*, 9939–9943; c) J. Liu, Y. Wang, G. Lei, J. Peng, Y. Huang, Y. Cao, M. Xie, X. Pu, Z. Lu, *J. Mater. Chem.* **2009**, *19*, 7753; d) P. Troselj, P. Bolgar, P. Ballester, C. A. Hunter, *J. Am. Chem. Soc.* **2021**, *143*, 8669–8678.

Manuscript received: November 24, 2022
Accepted manuscript online: January 10, 2023
Version of record online: ■■, ■■

Communications

Helical Structures

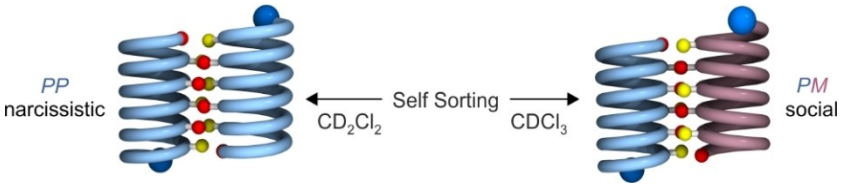

Aromatic foldamer helices form stable head-to-tail dimers in solution and in the solid state mediated by linear arrays of hydrogen bonds. The preference for dimerization between helices with opposite or identical handedness can be quantitatively reversed by the choice of chlorinated solvent.